ACADEMIC PRESS

Available online at www.sciencedirect.com

SCIENCE DIRECT®

Journal of Sound and Vibration 266 (2003) 217–234

JOURNAL OF SOUND AND VIBRATION

www.elsevier.com/locate/jsvi

Dynamic stability of two rigid rotors connected by a flexible coupling with angular misalignment

K.M. Al-Hussain*

Dynamic Analysis Unit, Saudi Aramco E-7180, Dhahran 31311, Saudi Arabia

Received 5 April 2002; accepted 9 September 2002

Abstract

The effect of misalignment on the stability of two rotors connected by a flexible mechanical coupling subjected to angular misalignment is examined. The study performed is to understand the effect of angular misalignment on the stability of rotating machinery. The dimensionless stability criteria of the non-linear system of differential equations of two misaligned rigid rotors are derived using Liapunov's direct method. A rigid disk is attached at the middle of each rotor, where the rotor–disk assembly is mounted on two hydrodynamic bearings with four stiffness and four damping coefficients. Sets of dimensionless conditions for sufficient whirl stability of the two misaligned rotors are derived. The stability conditions are presented in graphical form for deeper understanding of the effect of the flexible mechanical coupling stiffness and angular misalignment on rotating machinery stability. The results show that an increase in angular misalignment or mechanical coupling stiffness terms leads to an increase of the model stability region.

1. Introduction

The problem of misalignment as encountered in rotating machinery is of great concern to designers and maintenance engineers. It has been observed by the author on several occasions that rotating machinery stability conditions can change should the alignment state between the driver and the driven machines change. Due to the high speed of some rotating machinery, the need for a better understanding of the phenomena is becoming a necessity for practical engineers for the purpose of troubleshooting. Most rotating equipment consists of a driver and driven machine coupled through a mechanical coupling. Flexible mechanical couplings are becoming widely used in rotating machinery units. The mechanical coupling is used mainly to transmit torque from the driver to the driven machine. The two connected machines can go under misalignment, where severe

*Tel.: +9663-873-0311; fax: +9663-873-1023.
E-mail address: khaleel.hussain@aramco.com (K.M. Al-Hussain).

0022-460X/03/$ - see front matter
doi:10.1016/S0022-460X(02)01627-9

misalignment can cause high vibration to the machinery assembly. There are many publications on rotor stability, however, to the author's knowledge, there is little in the way of quantitative studies describing the coupling stiffness and misalignment effect on rotating equipment stability.

The application of flexible couplings for turbomachinery were discussed by Mancuso [1]. This reference includes reasons for using flexible couplings, difference between gear and flexible element couplings, and the selection of couplings for new applications. Lorenzen et al. [2] introduced a comparison of critical speeds of a high-speed compressor train alternatively equipped with different types of couplings. In this reference, the unbalance response using different types of couplings was calculated, which led to the conclusion that solid-type couplings can make the system more stable compared to other types of couplings. Rosenberg [3] presented the critical speed behavior of rotating shafts driven by universal couplings. It was shown that the model can develop mild instabilities at odd order integer submultiples of the critical speed. Al-Hussain and Redmond [4] studied the dynamic response of two Jeffcott rotors connected by rigid-type couplings with parallel misalignment. The study investigated the steady state and transient response of the system and concluded that the presence of lateral and torsional coupling are coupled. Sekhar and Prabhu [5] presented the effects of coupling misalignment on turbomachinery vibrations focusing on the effect of the location of the coupling with respect to the bending mode. Xu and Marangoni [6] presented a theoretical model of a complete motor rotor flexible coupling, discussing the system response under angular misalignment.

Saigo et al. [7] conducted theoretical and experimental investigations into the instability of a rotor system induced by coulomb friction in the universal joint. Nikolajsen [8] illustrated the large variation in the instability threshold speed, with radial bearing misalignment. He also showed how to determine the level of bearing misalignment that leads to optimum rotor stability. Chang and Cheng [9] analyzed the instability and non-linear dynamics of a slender rotating shaft with a rigid disk at the mid-span; the model studied is a simply supported shaft. Vance [10] discussed the response and stability of a single Jeffcott rotor on hydrodynamic bearings. He presented the whirl stability characteristics of hydrodynamic bearings as a function of the equilibrium eccentricity. A simplified approach to rotordynamic stability and concise analysis procedure for between-bearing rotors is presented by Stroh [11]. The technique combines the destabilizing effect and threshold value of excitation to evaluate the system stability.

The most common method, used in the literature, to derive stability criteria for rotor-bearing systems is by solving for the eigenvalues of the sets of equations of motion [12]. Lund [13] studied the nature of the eignenvalues for a uniform shaft supported at the ends by damped bearings. The Routh–Hurwitz criterion is also commonly used to study the stability of linearized rotor-bearing system, as presented by Dimarogonas and Haddad [14]. The procedure for using the Routh–Hurwitz criterion requires the system characteristic equation with linear coefficients. The use of Liapunov's direct method to evaluate the dynamic and parametric stability of elastic and rigid rotors-bearing systems in the neighborhood of equilibrium is used by El-Marhomy and Schlack [15,16]. They showed quantitatively the effect of different shaft and bearing parameters on the stability regions. Meirovitch [17] presented Liapunov's direct method to determine the dynamic system stability characteristics without solving the system differential equations. Numerical investigations are often time adopted to study the stability of rigid rotors supported in plain bearings [18].

To this end, one can summarize that few studies have covered the detailed approach of analyzing the effect of angular misalignment on rotating machinery stability. To the knowledge of

the authors, no study has quantified the effect of coupling angular misalignment on the stability of rotating machinery, which had been experienced in rotating machinery on a number of occasions.

The present work is devoted toward the analysis of stability due to angular misalignment, to aid practical rotating equipment engineers to gain inclusive understanding of the role played by misalignment and other parameters on the stability of the system under study. The need of this study is coming from the author's field experience that the alignment condition can affect the rotating machine stability. The work starts by introducing a simple model that consists of two rigid rotors mounted on hydrodynamic bearings that contain principal and cross-coupling stiffness and damping terms. Due to the non-linearity of the system, the dimensionless stability criteria are derived using Liapunov's direct method. To gain a greater insight of the effect of angular misalignment on stability, graphical presentations for different dimensionless stability parameters are presented.

2. The dynamic model

2.1. System descriptions and assumptions

Two disks m_1 and m_2 are each mounted at the center of two rigid rotors that are connected through a flexible-type coupling. The two shafts are initially in a state of angular misalignment of magnitude α, as shown in Fig. 1. The two shafts are rigid and have lengths of l_1 and l_2.

Each rotor is supported by two hydrodynamic bearings with eight coefficients of stiffness and damping, including cross-coupling terms, as shown in Fig. 2. The x_p, y_p, z_p rotating co-ordinates are located at the centers of the mass with unit vectors $\mathbf{i}_p, \mathbf{j}_p, \mathbf{k}_p$, respectively.

For simplification purposes, it is assumed that the two rotors are misaligned, with a static angular misalignment α. Assuming small angular displacements, the position vectors at different locations on the shafts described in Fig. 1 can be represented by

$$\mathbf{r}_{mp} = x_p\mathbf{i}_p + y_p\mathbf{j}_p + z_p\mathbf{k}_p, \tag{1}$$

where p indicates shaft 1 or 2:

$$\mathbf{r}_{bp1} = \left(x_p - \frac{l_p}{2}\theta_p\right)\mathbf{i}_p + \left(y_p - \frac{l_p}{2}\phi_p\right)\mathbf{j}_p + \left(z_p - \frac{l_p}{2}\right)\mathbf{k}_p, \tag{2}$$

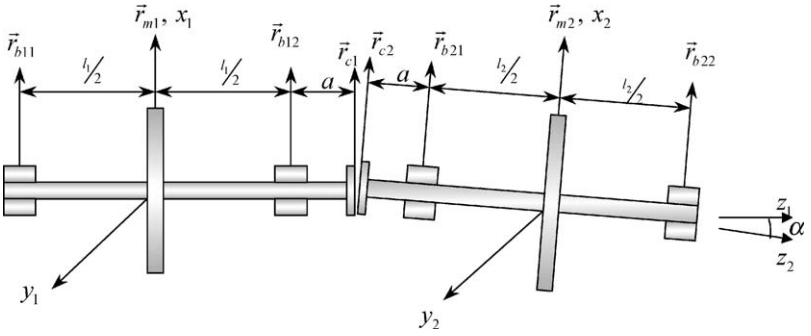

Fig. 1. Two attached mass rigid rotors with angular misalignment.

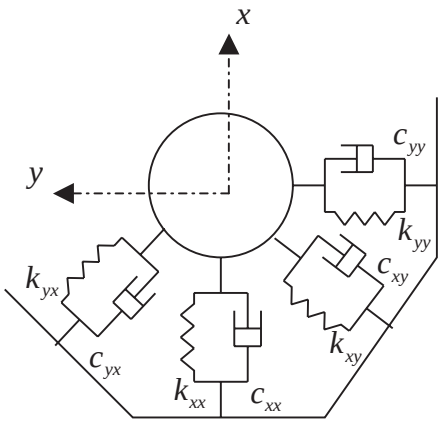

Fig. 2. Support stiffness and damping coefficients.

$$\mathbf{r}_{bp2} = \left(x_p + \frac{l_p}{2}\theta_p\right)\mathbf{i}_p + \left(y_p + \frac{l_p}{2}\phi_p\right)\mathbf{j}_p + \left(z_p + \frac{l_p}{2}\right)\mathbf{k}_p, \tag{3}$$

$$\mathbf{r}_{cp} = \left\{x_p + \left(\frac{l_p}{2} + a\right)\theta_p\right\}\mathbf{i}_p + \left\{y_p + \left(\frac{l_p}{2} + a\right)\phi_p\right\}\mathbf{j}_p + \left\{z_p + \left(\frac{l_p}{2} + a\right)\right\}\mathbf{k}_p. \tag{4}$$

The two disks are assumed rigid and their instantaneous angular velocities are

$$\boldsymbol{\omega}_p = \omega_{xp}\mathbf{i}_2 + \omega_{yp}\mathbf{j}_p + \omega_{zp}\mathbf{k}_p, \tag{5}$$

$$\begin{bmatrix}\omega_{xp}\\ \omega_{yp}\\ \omega_{zp}\end{bmatrix} = \begin{bmatrix}\dot{\phi}_p - \dot{\beta}_p \sin\theta_p\\ \dot{\theta}_p \cos\phi_p - \dot{\beta}_p \cos\theta_p \sin\phi_p\\ \dot{\beta}_p \cos\theta_p \cos\phi_p + \dot{\phi}_p \sin\theta_p\end{bmatrix}, \tag{6}$$

where ϕ in the x direction, θ in the y direction, and β in the z direction. By linearizing Eq. (6), neglecting the higher terms, the angular velocities become

$$\begin{bmatrix}\omega_{xp}\\ \omega_{yp}\\ \omega_{zp}\end{bmatrix} = \begin{bmatrix}\dot{\phi}_p - \dot{\beta}_p\theta_p\\ \dot{\theta}_p - \dot{\beta}_p\phi_p\\ \dot{\beta}_p + \theta_p\dot{\phi}_p\end{bmatrix}. \tag{7}$$

Using co-ordinate transformation, the coupling hub position $\mathbf{r}_{c2}$, of rotor 2, can be expressed in terms of rotor 1 unit vectors for use in a potential energy expression

$$\begin{aligned}\mathbf{r}_{c2} = &\left[\left\{x_2 - \left(\frac{l_2}{2} + a\right)\theta_2\right\}\cos\alpha - \left\{z_2 - \left(\frac{l_2}{2} + a\right)\right\}\sin\alpha\right]\mathbf{i}_1 + \left\{y_2 - \left(\frac{l_2}{2} + a\right)\phi_2\right\}\mathbf{j}_1\\ &\times\left[\left\{x_2 - \left(\frac{l_2}{2} + a\right)\theta_2\right\}\sin\alpha + \left\{z_2 - \left(\frac{l_2}{2} + a\right)\right\}\cos\alpha\right]\mathbf{k}_1.\end{aligned} \tag{8}$$

2.2. Kinetic, potential, and dissipation energy expressions

It is assumed that the two shafts are massless and have the same lengths and mounted on similar bearings. The total kinetic energy expression of the two rotors become

$$T = \frac{1}{2}\sum_{p=1}^{2}\{m_p\dot{\mathbf{r}}_{mp}\cdot\dot{\mathbf{r}}_{mp} + I_{Dp}(\omega_{xp}^2+\omega_{yp}^2) + I_{Pp}\omega_{zp}^2\}. \tag{9}$$

The generalized co-ordinates of the model under consideration can be expressed as

$$\mathbf{q} = \{x_1, y_1, \phi_1, \theta_1, x_2, y_2, \phi_2, \theta_2, z_1, z_2\}. \tag{10}$$

Carrying the time derivative of the unit vector $\dot{\mathbf{r}}_{mp}$, substituting in Eq. (9), and using the angular velocity expressions designated by Eq. (7), the total kinetic energy becomes

$$\begin{aligned} T = \frac{1}{2}\sum_{p=1}^{2}&\{m_p\{\dot{x}_p - y_p(\dot{\beta}_p+\dot{\phi}_p\theta_p) - z_p(\dot{\theta}_p-\dot{\beta}_p\phi_p)\}^2 + \{\dot{y}_p - x_p(\dot{\beta}_p+\dot{\phi}_p\theta_p)\\ &- z_p(\dot{\phi}_p-\dot{\beta}_p\theta_p)\}^2 + \{\dot{z}_p - x_p(\dot{\theta}_p-\dot{\beta}_p\phi_p) + y_p(\dot{\phi}_p-\dot{\beta}_p\theta_p)\}^2\\ &+ I_{Dp}\{(\dot{\phi}_p-\dot{\beta}_p\theta_p)^2 + (\dot{\theta}_p-\dot{\beta}_p\phi_p)^2\} + I_{Pp}(\dot{\beta}_p+\dot{\phi}_p\theta_p)^2\}. \end{aligned} \tag{11}$$

For simplification purposes, assume all bearings are similar and both shafts have the same lengths $l_1 = l_2$. Utilizing the position vectors of Eqs. (2)–(4), the potential energy for the total assembly can be given as

$$\begin{aligned} V &= \frac{1}{2}\sum_i\sum_j k_{ij}q_iq_j\\ &= \sum_{p=1}^{2}\left[\frac{1}{2}k_{xx}\left\{\left(x_p-\frac{l}{2}\theta_p\right)^2+\left(x_p+\frac{l}{2}\theta_p\right)^2\right\}.\right.\\ &\quad+\frac{1}{2}k_{yy}\left\{\left(y_p-\frac{l}{2}\phi_p\right)^2+\left(y_p+\frac{l}{2}\phi_p\right)^2\right\}\\ &\quad+\frac{1}{2}k_{xy}\left\{\left(x_p-\frac{l}{2}\theta_p\right)\left(y_p-\frac{l}{2}\phi_p\right)+\left(x_p+\frac{l}{2}\theta_p\right)\left(y_p+\frac{l}{2}\phi_p\right)\right\}\\ &\quad\left.+\frac{1}{2}k_{yx}\left\{\left(x_p-\frac{l}{2}\theta_p\right)\left(y_p-\frac{l}{2}\phi_p\right)+\left(x_p+\frac{l}{2}\theta_p\right)\left(y_p+\frac{l}{2}\phi_p\right)\right\}\right]\\ &\quad+k_{cx}\left[(x_1-x_2\cos\alpha)+\left(\frac{l}{2}+a\right)(\theta_1+\theta_2\cos\alpha)+\left\{z_2-\left(\frac{l}{2}+a\right)\right\}\sin\alpha\right]^2 \end{aligned}$$

$$+k_{cy}\left[(y_1-y_2)+\left\{\left(\frac{l}{2}+a\right)(\phi_1+\phi_2\sin\alpha)\right\}\right]^2$$
$$+k_{cz}\left[(z_1-z_2\cos\alpha)+\left\{\left(\frac{l}{2}+a\right)(1+\cos\alpha)\right\}-\left\{x_2+\left(\frac{l}{2}+a\right)\theta_2\right\}\sin\alpha\right]^2$$
$$+k_{c\phi}(\phi_1-\phi_2\cos\alpha+\beta_2\sin\alpha)^2+k_{c\theta}(\theta_1-\theta_2)^2+k_{c\beta}(\beta_1-\phi_2\sin\alpha-\beta_2\cos\alpha)^2. \quad (12)$$

Since the model assembly is fitted with the same bearings in all designated locations, Fig. 1, and the damping cross-coupling terms of each bearing are equal $c_{xy}=c_{yx}$, the energy dissipation due to bearing damping can be written as

$$D=\frac{1}{2}\sum_i\sum_j c_{ij}\dot{q}_i\dot{q}_j$$
$$=\sum_{p=1}^{2}\left[\frac{1}{2}C_{xx}\left\{\left(\dot{x}_p-\frac{l}{2}\dot{\theta}_p\right)^2+\left(\dot{x}_p+\frac{l}{2}\dot{\theta}_p\right)^2\right\}.\right.$$
$$+\frac{1}{2}C_{yy}\left\{\left(\dot{y}_p-\frac{l}{2}\dot{\phi}_p\right)^2+\left(\dot{y}_p+\frac{l}{2}\dot{\phi}_p\right)^2\right\}$$
$$\left.+C_{xy}\left\{\left(\dot{x}_p-\frac{l}{2}\dot{\theta}_p\right)\left(\dot{y}_p-\frac{l}{2}\dot{\phi}_p\right)+\left(\dot{x}_p+\frac{l}{2}\dot{\theta}_p\right)\left(\dot{y}_p+\frac{l}{2}\dot{\phi}_p\right)\right\}\right]. \quad (13)$$

Eq. (13) shows that angular misalignment has no influence on the dissipated energy and the effect of dissipated energy on stability is well covered in the literature; therefore, it is omitted from this work.

2.3. Stability condition due to system stiffness and gyroscopic effects

Since the system can be described by the Lagrangian $L=T-V$ where T is the kinetic energy of the system and V is the potential energy of the system. The general form of the kinetic energy can be expressed as

$$T(\mathbf{q},\dot{\mathbf{q}})=\tfrac{1}{2}\dot{\mathbf{q}}^{\mathrm{T}}\mathbf{A}(\mathbf{q})\dot{\mathbf{q}}+\mathbf{B}(\mathbf{q})\dot{\mathbf{q}}+C(\mathbf{q}). \quad (14)$$

For a conservative system, the Hamiltonian, which can be written as $H=T_2-T_0+V$ may be used as a Liapunov's function in the region of equilibrium that is $q_i=\dot{q}_i=0$, where $T_2=\frac{1}{2}\dot{\mathbf{q}}^{\mathrm{T}}\mathbf{A}(\mathbf{q})\dot{\mathbf{q}}$, $T_1=\mathbf{B}(\mathbf{q})\dot{\mathbf{q}}, T_0=C(q)$ labelled according to the power of $\dot{\mathbf{q}}$. Since T_2 is a positive function of the generalized velocities, then the remaining terms of the Hamiltonian $U=-T_0+V$ can be checked for the sign definite in the region of equilibrium to determine the stability criteria of the conservative system. Therefore, U can be considered as Liapunov's function and if it is a positive definite function of the generalized co-ordinates in the neighborhood of equilibrium, then the system is stable.

To simplify the solution further, it is assumed that the assembly rotational velocity is constant, $\dot{\beta}=\Omega$, neglecting the small variation in the rotating speed, and angular misalignment α is small.

The potential energy equation can be simplified to

$$
\begin{aligned}
U = \sum_{p=1}^{2} \Bigg[& \frac{1}{2}k_{xx}\left\{\left(x_p - \frac{l}{2}\theta_p\right)^2 + \left(x_p + \frac{l}{2}\theta_p\right)^2\right\} \\
& + \frac{1}{2}k_{xy}\left\{\left(x_p - \frac{l}{2}\theta_p\right)\left(y_p - \frac{l}{2}\phi_p\right) + \left(x_p + \frac{l}{2}\theta_p\right)\left(y_p + \frac{l}{2}\phi_p\right)\right\} \\
& + \frac{1}{2}k_{yx}\left\{\left(x_p - \frac{l}{2}\theta_p\right)\left(y_p - \frac{l}{2}\phi_p\right) + \left(x_p + \frac{l}{2}\theta_p\right)\left(y_p + \frac{l}{2}\phi_p\right)\right\} \\
& + \frac{1}{2}k_{yy}\left\{\left(y_p - \frac{l}{2}\phi_p\right)^2 + \left(y_p + \frac{l}{2}\phi_p\right)^2\right\}\Bigg] \\
& + k_{cx}\left[(x_1 - x_2) + \left(\frac{l}{2} + a\right)(\theta_1 + \theta_2) + \left\{z_2 - \left(\frac{l}{2} + a\right)\right\}\alpha\right]^2 \\
& + k_{cy}\left[(y_1 - y_2) + \left\{\left(\frac{l}{2} + a\right)(\phi_1 + \phi_2\alpha)\right\}\right]^2 \\
& + k_{cz}\left[(z_1 - z_2) + \left\{\left(\frac{l}{2} + a\right)(2)\right\} - \left\{x_2 + \left(\frac{l}{2} + a\right)\theta_2\right\}\alpha\right]^2 \\
& + k_{c\phi}(\phi_1 - \phi_2)^2 + k_{c\theta}(\theta_1 - \theta_2)^2 + k_{c\beta}(\phi_2\alpha)^2 \\
& \sum_{p=1}^{2}\Bigg[-\frac{1}{2}m_p\{(y_p\Omega - z_p\Omega\phi_p)^2 + (x_p\Omega - z_p\Omega\theta_p)^2 + (x_p\phi_p\Omega - y_p\Omega\theta_p)^2\} \\
& - \frac{1}{2}I_{Dp}(\Omega^2\theta_p^2 + \Omega^2\phi_p^2) - \frac{1}{2}I_{Pp}\Omega^2\Bigg].
\end{aligned}
\tag{15}
$$

Successive partial derivatives of U with respect to the generalized co-ordinates $\mathbf{q} = \{x_1, y_1, \phi_1, \theta_1, x_2, y_2, \phi_2, \theta_2, z_1, z_2\}$, evaluating each derivative at equilibrium, to form the following Hessian matrix:

$$
\mathbf{Q} = \left[\begin{array}{cccc}
\dfrac{\partial^2 U}{\partial q_1\,\partial q_1} & \dfrac{\partial^2 U}{\partial q_1\,\partial q_2} & \cdots & \dfrac{\partial^2 U}{\partial q_1\,\partial q_n} \\
\dfrac{\partial^2 U}{\partial q_2\,\partial q_1} & \dfrac{\partial^2 U}{\partial q_2\,\partial q_2} & \cdots & \dfrac{\partial^2 U}{\partial q_2\,\partial q_n} \\
\vdots & \vdots & \vdots & \vdots \\
\dfrac{\partial^2 U}{\partial q_n\,\partial q_1} & \dfrac{\partial^2 U}{\partial q_n\,\partial q_1} & \cdots & \dfrac{\partial^2 U}{\partial q_n\,\partial q_n}
\end{array}\right]_{q=\dot{q}=0}. \tag{16}
$$

If the Hessian matrix **Q** is positive definite at equilibrium, then the system is stable. Neglecting the rows and columns for the z co-ordinates and setting $\gamma = 2(1/2\,l + a)$ the matrix becomes

$$\mathbf{Q} = \begin{bmatrix} Q_{11} & k_{xy}+k_{yx} & 0 & \gamma k_{cx} & -2k_{cx} & 0 & 0 & \gamma k_{cx} \\ k_{xy}+k_{yx} & Q_{22} & \gamma k_{cy} & 0 & 0 & -2k_{cy} & \gamma\alpha k_{cy} & 0 \\ 0 & \gamma k_{cy} & Q_{33} & \frac{1}{4}l^2(k_{xy}+k_{yx}) & 0 & -\gamma k_{cy} & Q_{37} & 0 \\ \gamma k_{cx} & 0 & \frac{1}{4}l^2(k_{xy}+k_{xy}) & Q_{44} & -\gamma k_{cx} & 0 & 0 & Q_{48} \\ -2k_{cx} & 0 & 0 & -\gamma k_{cx} & Q_{55} & k_{xy}+k_{yx} & 0 & Q_{58} \\ 0 & -2k_{cy} & -\gamma k_{cy} & 0 & k_{xy}+k_{yx} & Q_{66} & -\gamma\alpha k_{cy} & 0 \\ 0 & \gamma\alpha k_{cy} & Q_{73} & 0 & 0 & -\gamma\alpha k_{cy} & Q_{77} & \frac{1}{4}l^2(k_{xy}+k_{yx}) \\ \gamma k_{cx} & 0 & 0 & Q_{84} & Q_{85} & 0 & \frac{1}{4}l^2(k_{xy}+k_{yx}) & Q_{88} \end{bmatrix}, \tag{17}$$

where the matrix entries

$$Q_{11} = 2(k_{xx}+k_{cx}) - m_1\Omega^2, \tag{18}$$

$$Q_{22} = 2(k_{yy}+k_{cy}) - m_1\Omega^2, \tag{19}$$

$$Q_{33} = \tfrac{1}{2}l^2k_{yy} + \gamma^2k_{cy} + 2k_{c\phi} - I_{D1}\Omega^2, \tag{20}$$

$$Q_{44} = \tfrac{1}{2}l^2k_{xx} + \gamma^2k_{cx} + 2k_{c\theta} - I_{D1}\Omega^2, \tag{20'}$$

$$Q_{55} = 2(k_{xx}+k_{cx}+\alpha^2k_{cz}) - m_2\Omega^2, \tag{21}$$

$$Q_{66} = 2(k_{yy}+k_{cy}) - m_2\Omega^2, \tag{22}$$

$$Q_{77} = \tfrac{1}{2}l^2k_{yy} + \gamma^2\alpha^2k_{cy} + 2k_{c\phi} + 2\alpha^2k_{c\beta} - I_{D2}\Omega^2, \tag{23}$$

$$Q_{88} = \tfrac{1}{2}l^2k_{xx} + \gamma^2\alpha^2k_{cz} + 2k_{c\theta} - I_{D2}\Omega^2, \tag{24}$$

$$Q_{37} = Q_{73} = \gamma^2\alpha k_{cy} - 2k_{c\phi}, \tag{25}$$

$$Q_{48} = Q_{84} = \gamma^2k_{cx} - 2k_{c\theta}, \tag{26}$$

$$Q_{58} = Q_{85} = \gamma(k_{cx} - \alpha k_{cz}). \tag{27}$$

To simplify the matrix further, keeping the parameters that lead to the understanding of the angular misalignment effect, assume

$$m_1 = m_2 = m, \qquad I_{D1} = I_{D2} = I.$$

Dividing **Q** by $m\Omega^2$, and introducing

$$\omega_{c\phi}^2 = \frac{k_{c\phi}}{ml^2}, \quad \omega_{c\theta}^2 = \frac{k_{c\theta}}{ml^2} \quad \text{and} \quad \omega_{ij}^2 = \frac{k_{ij}}{m}$$

the **Q** matrix becomes dimensionless, $\mathbf{Q}^*$.

$$\mathbf{Q}^* = \begin{bmatrix}
Q_{11}^* & \left(\frac{\omega_{xy}^2+\omega_{yx}^2}{\Omega^2}\right) & 0 & \gamma\left(\frac{\omega_{cx}^2}{\Omega^2}\right) & -2\left(\frac{\omega_{cx}^2}{\Omega^2}\right) & 0 & 0 & \gamma\left(\frac{\omega_{cx}^2}{\Omega^2}\right) \\
\left(\frac{\omega_{xy}^2+\omega_{yx}^2}{\Omega^2}\right) & Q_{22}^* & \gamma\left(\frac{\omega_{cy}^2}{\Omega^2}\right) & 0 & 0 & -2\left(\frac{\omega_{cy}^2}{\Omega^2}\right) & \gamma\alpha\left(\frac{\omega_{cy}^2}{\Omega^2}\right) & 0 \\
0 & \gamma\left(\frac{\omega_{cy}^2}{\Omega^2}\right) & Q_{33}^* & \frac{1}{4}l^2\left(\frac{\omega_{xy}^2+\omega_{yx}^2}{\Omega^2}\right) & 0 & -\gamma\left(\frac{\omega_{cy}^2}{\Omega^2}\right) & Q_{37}^* & 0 \\
\gamma\left(\frac{\omega_{cx}^2}{\Omega^2}\right) & 0 & \frac{1}{4}l^2\left(\frac{\omega_{xy}^2+\omega_{yx}^2}{\Omega^2}\right) & Q_{44}^* & -\gamma\left(\frac{\omega_{cx}^2}{\Omega^2}\right) & 0 & 0 & Q_{48}^* \\
-2\left(\frac{\omega_{cx}^2}{\Omega^2}\right) & 0 & 0 & -\gamma\left(\frac{\omega_{cx}^2}{\Omega^2}\right) & Q_{55}^* & \left(\frac{\omega_{xy}^2+\omega_{yx}^2}{\Omega^2}\right) & 0 & Q_{58}^* \\
0 & -2k_{cy}\left(\frac{\omega_{cy}^2}{\Omega^2}\right) & -\gamma\left(\frac{\omega_{cy}^2}{\Omega^2}\right) & 0 & \left(\frac{\omega_{xy}^2+\omega_{yx}^2}{\Omega^2}\right) & Q_{66}^* & -\gamma\alpha\left(\frac{\omega_{cy}^2}{\Omega^2}\right) & 0 \\
0 & \gamma\alpha\left(\frac{\omega_{cy}^2}{\Omega^2}\right) & Q_{73}^* & 0 & 0 & -\gamma\alpha\left(\frac{\omega_{cy}^2}{\Omega^2}\right) & Q_{77}^* & \frac{1}{4}l^2\left(\frac{\omega_{xy}^2+\omega_{yx}^2}{\Omega^2}\right) \\
\gamma\left(\frac{\omega_{cx}^2}{\Omega^2}\right) & 0 & 0 & Q_{84}^* & Q_{85}^* & 0 & \frac{1}{4}l^2\left(\frac{\omega_{xy}^2+\omega_{yx}^2}{\Omega^2}\right) & Q_{88}^*
\end{bmatrix}. \tag{28}$$

Matrix entries presented in Eqs. (18)–(27) can be written in dimensionless form

$$Q_{11}^{*} = 2\left(\frac{\omega_{xx}^2 + \omega_{cx}^2}{\Omega^2}\right) - 1, \tag{29}$$

$$Q_{22}^{*} = 2\left(\frac{\omega_{yy}^2 + \omega_{cy}^2}{\Omega^2}\right) - 1, \tag{30}$$

$$Q_{33}^{*} = l^2\left(\frac{1}{2}\left(\frac{\omega_{yy}^2}{\Omega^2}\right) + \frac{\gamma^2}{l^2}\left(\frac{\omega_{cy}^2}{\Omega^2}\right) + 2\left(\frac{\omega_{c\phi}^2}{\Omega^2}\right) - \frac{I}{ml^2}\right), \tag{31}$$

$$Q_{44}^{*} = l^2\left(\frac{1}{2}\left(\frac{\omega_{xx}^2}{\Omega^2}\right) + \frac{\gamma^2}{l^2}\left(\frac{\omega_{cx}^2}{\Omega^2}\right) + 2\left(\frac{\omega_{c\theta}^2}{\Omega^2}\right) - \frac{I}{ml^2}\right), \tag{32}$$

$$Q_{55}^{*} = \left(2\left[\left(\frac{\omega_{xx}^2}{\Omega^2}\right) + \left(\frac{\omega_{cx}^2}{\Omega^2}\right) + \alpha^2\left(\frac{\omega_{cz}^2}{\Omega^2}\right)\right] - 1\right), \tag{33}$$

$$Q_{66}^{*} = \left(2\left[\left(\frac{\omega_{yy}^2}{\Omega^2}\right) + \left(\frac{\omega_{cy}^2}{\Omega^2}\right)\right] - 1\right), \tag{34}$$

$$Q_{77}^{*} = l^2\left(\frac{1}{2}\left(\frac{\omega_{yy}^2}{\Omega^2}\right) + \frac{\gamma^2\alpha^2}{l^2}\left(\frac{\omega_{cy}^2}{\Omega^2}\right) + 2\left(\frac{\omega_{c\phi}^2}{\Omega^2}\right) - \frac{I}{ml^2}\right), \tag{35}$$

$$Q_{88}^{*} = l^2\left(\frac{1}{2}\left(\frac{\omega_{xx}^2}{\Omega^2}\right) + \frac{\gamma^2\alpha^2}{l^2}\left(\frac{\omega_{cz}^2}{\Omega^2}\right) + 2\left(\frac{\omega_{c\theta}^2}{\Omega^2}\right) - \frac{I}{ml^2}\,\Omega^2\right), \tag{36}$$

$$Q_{37}^{*} = Q_{73}^{*} = \gamma^2\alpha\left(\frac{\omega_{cy}^2}{\Omega^2}\right) - 2\left(\frac{\omega_{c\phi}^2}{\Omega^2}\right), \tag{37}$$

$$Q_{48}^{*} = Q_{84}^{*} = \gamma^2\left(\frac{\omega_{cx}^2}{\Omega^2}\right) - 2\left(\frac{\omega_{c\theta}^2}{\Omega^2}\right), \tag{38}$$

$$Q_{58}^{*} = Q_{85}^{*} = \gamma\left(\left(\frac{\omega_{cx}^2}{\Omega^2}\right) - \alpha\left(\frac{\omega_{cz}^2}{\Omega^2}\right)\right). \tag{39}$$

By setting $\mu = I/ml^2$ and $\gamma^2/l^2 = 1$, the conditions for sufficient stability for the misaligned model under study are the conditions that make the Hermitian matrix $\mathbf{Q}$ positive definite. If we assume that the dimensionless Hermitian matrix is positive definite then all of the diagonal elements are positive and $Q_{ii}^{*}Q_{jj}^{*} > |Q_{ij}^{*}|^2$, for distinct i and j. The following conditions are sufficient condition for the model to become asymptotically stable, providing $|Q| > 0$.

$$\left(\frac{\omega_{xx}^2 + \omega_{cx}^2}{\Omega^2}\right) > \frac{1}{2}, \tag{40}$$

$$\left(\left(\frac{\omega_{xx}^2+\omega_{cx}^2}{\Omega^2}\right)-\frac{1}{2}\right)\left(\left(\frac{\omega_{yy}^2+\omega_{cy}^2}{\Omega^2}\right)-\frac{1}{2}\right)>\frac{1}{4}\left(\frac{\omega_{xy}^2+\omega_{yx}^2}{\Omega^2}\right)^2, \tag{41}$$

$$\left(\left(\frac{\omega_{yy}^2}{\Omega^2}\right)+2\left(\frac{\omega_{cy}^2}{\Omega^2}\right)+4\left(\frac{\omega_{c\phi}^2}{\Omega^2}\right)-2\mu\right)>0, \tag{42}$$

$$\left(\left(\frac{\omega_{yy}^2}{\Omega^2}\right)+2\left(\frac{\omega_{cy}^2}{\Omega^2}\right)+4\left(\frac{\omega_{c\phi}^2}{\Omega^2}\right)-2\mu\right)\left(\left(\frac{\omega_{xx}^2}{\Omega^2}\right)+2\left(\frac{\omega_{cx}^2}{\Omega^2}\right)+4\left(\frac{\omega_{c\theta}^2}{\Omega^2}\right)-2\mu\right)>\frac{1}{4}\left(\frac{\omega_{xy}^2+\omega_{yx}^2}{\Omega^2}\right)^2, \tag{43}$$

$$\left(\left(\frac{\omega_{xx}^2}{\Omega^2}\right)+\left(\frac{\omega_{cx}^2}{\Omega^2}\right)+\alpha^2\left(\frac{\omega_{cz}^2}{\Omega^2}\right)-\frac{1}{2}\right)>0, \tag{44}$$

$$\left(\left(\frac{\omega_{xx}^2}{\Omega^2}\right)+\left(\frac{\omega_{cx}^2}{\Omega^2}\right)+\alpha^2\left(\frac{\omega_{cz}^2}{\Omega^2}\right)-\frac{1}{2}\right)\left(\left(\frac{\omega_{yy}^2}{\Omega^2}\right)+\left(\frac{\omega_{cy}^2}{\Omega^2}\right)-\frac{1}{2}\right)>\frac{1}{4}\left(\frac{\omega_{xy}^2+\omega_{yx}^2}{\Omega^2}\right)^2, \tag{45}$$

$$\left(\left(\frac{\omega_{yy}^2}{\Omega^2}\right)+2\alpha^2\left(\frac{\omega_{cy}^2}{\Omega^2}\right)+4\left(\frac{\omega_{c\phi}^2}{\Omega^2}\right)-2\mu\right)>0, \tag{46}$$

$$\left(\left(\frac{\omega_{yy}^2}{\Omega^2}\right)+2\alpha^2\left(\frac{\omega_{cy}^2}{\Omega^2}\right)+4\left(\frac{\omega_{c\phi}^2}{\Omega^2}\right)-2\mu\right)\times\left(\left(\frac{\omega_{xx}^2}{\Omega^2}\right)+2\alpha^2\left(\frac{\omega_{cz}^2}{\Omega^2}\right)+4\left(\frac{\omega_{c\theta}^2}{\Omega^2}\right)-2\mu\right)>\frac{1}{4}\left(\frac{\omega_{xy}^2+\omega_{yx}^2}{\Omega^2}\right)^2. \tag{47}$$

These stability criteria determine the conditions for the system to be stable. In Eqs. (44)–(47), the square of angular misalignment is a multiplication factor for one of the coupling stiffness coefficients, increasing angular misalignment causes an increase in the system principal stiffness coefficients.

3. Presentation of results and discussion

Eqs. (40)–(47) represent conditions for whirl stability of the two rigid rotors connected through a flexible mechanical coupling with angular misalignment. All of these stability conditions show that the coupling dimensionless parameters (DP) and angular misalignment play a major role in the stability of the model. The bearing principal and cross-coupling DP are functions of the hydrodynamic characteristics which are obtained from the solution of Reynolds' equation. The solution gives stiffness and viscous damping coefficients in dimensionless form as a function of Sommerfeld number [10].

The stability condition (40) shows that coupling DP component is added to the bearing principal DP in the x direction; this is a result of the addition of the bearing principal stiffness and

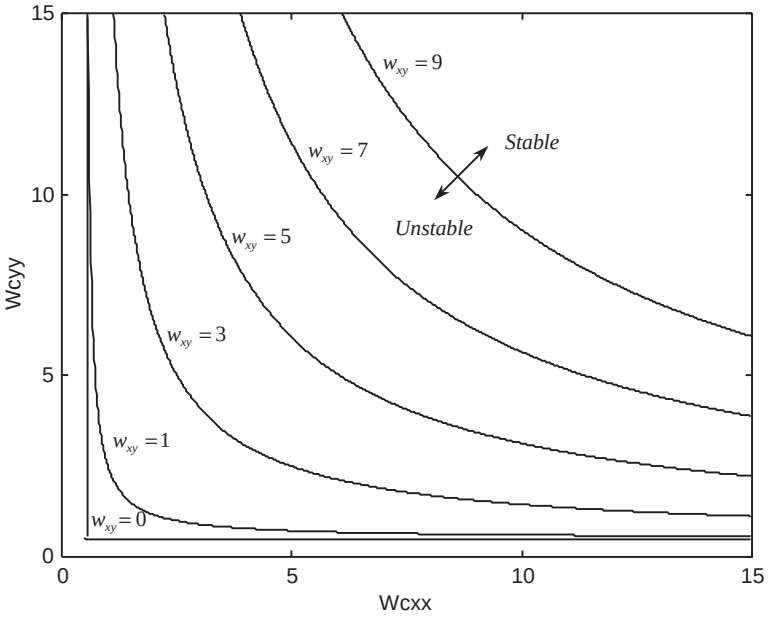

Fig. 3. Bearing cross-coupling term effects on the stability region.

coupling stiffness terms in the x and y directions. The condition expression indicates that the combined bearing principal and coupling DP in the x direction needs to be greater than $\frac{1}{2}$, to maintain stability of the model under study.

Eq. (41) represents the second stability criteria; combining the coupling stiffness with the bearing principal stiffness and assuming they are equal for the purpose of demonstration, the equation reduces to $(Wcxx - 1/2)(Wcyy - 1/2) > Wxy^2$, where $Wcxx = (\omega_{xx}^2 + \omega_{cx}^2)/\Omega^2$, $Wcyy = (\omega_{yy}^2 + \omega_{cy}^2)/\Omega^2$, and $Wxy = (\omega_{xy}^2 + \omega_{yx}^2)/2\Omega^2$. Fig. 3 clearly demonstrates the influence of the bearing cross-coupling DP on the model stability. The different curves in Fig. 3 are for different values of the bearing cross-coupling terms, this indicates that the stability region reduces as the cross-coupling DP increases. For the case that the cross-coupling DP term, Wxy is zero, the stability threshold becomes $\frac{1}{2}$.

Eq. (42) depends on coupling radial DP for the y and ϕ directions and the bearing principal DP in the y direction. The threshold of stability is a function of the dimensionless parameter 2μ. To simplify the presentation of this condition, assume that the dimensionless coupling stiffness parameters are equal to $\omega_{cy\phi}^2/\Omega^2$, the condition reduces to $Wyy = 2\mu - 6Wcyp$, if it assumed that $Wyy = \omega_{yy}^2/\Omega^2$, $6\ Wcyp = 2(\omega_{cy}^2/\Omega^2) + 4(\omega_{c\phi}^2/\Omega^2)$, and $\omega_{cy}^2/\Omega^2 = \omega_{c\phi}^2/\Omega^2$. The variation of the stability region depends on the value of μ as shown in Fig. 4. Increasing the disk transverse moment of inertia, decreasing the mass or the shaft length increases μ, this leads to the reduction of the stability region. It is obvious that increasing the coupling DP, which depends on the coupling stiffness leads to making the system more stable.

Eq. (43) combines the effect of the bearing and coupling DPs, where threshold stability depends on the dimensionless term μ. Assuming the DPs are all equal, then the equation

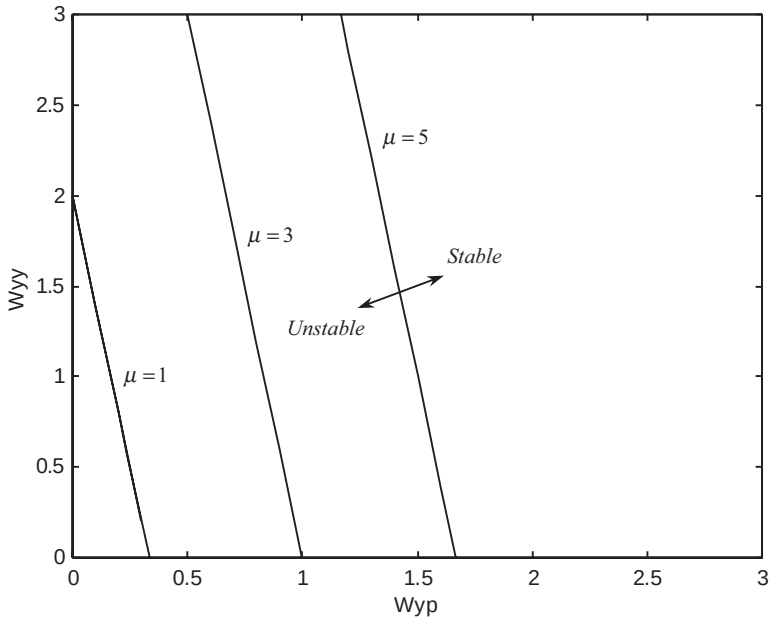

Fig. 4. Effect of the dimensionless termμ, Eq. (42).

can be simplified to $(Wcy\phi - 2\mu)(Wcx\theta - 2\mu) = Wxy^2$, assuming $Wcy\phi = (\omega_{yy}^2/\Omega^2) + 2(\omega_{cy}^2/\Omega^2) + 4(\omega_{c\phi}^2/\Omega^2)$, $Wcx\theta = (\omega_{xx}^2/\Omega^2) + 2(\omega_{cx}^2/\Omega^2) + 4(\omega_{c\theta}^2/\Omega^2)$, and $Wxy = \omega_{xy}^2 + \omega_{yx}^2/2\Omega^2$. Graphical presentation of this equation is shown in Fig. 5. As expected, the stability region decreases as the dimensionless term μ increases.

Eqs. (44)–(47) are directly dependent on the model angular misalignment α. In practical terms a flexible-type coupling may not tolerate more than 1° (17.5 mrad) of angular misalignment, this amount of misalignment will cause excessive dynamic forces on the bearings. However, the study is intended to determine the stability sensitivity to angular misalignment in dimensionless form. Eq. (44) indicates that introducing an angular misalignment tends to directly increase the system principal DP, and makes the system more stable.

The stability condition presented by Eq. (45) can be simplified in similar way to $(Wcxz - 1/\lambda)(Wcyy - 1/4) = Wxy^2/\lambda$, by setting $Wcxz = \omega_{xx}^2/\Omega^2 = \omega_{cx}^2/\Omega^2 = \omega_{cz}^2/\Omega^2$, $Wcyy = \omega_{yy}^2/\Omega^2 = \omega_{cy}^2/\Omega^2$, $Wxy = \omega_{xy}^2 + \omega_{yx}^2/2\Omega^2$, and $\lambda = 2(2 + \alpha^2)$, to demonstrate the effect of angular misalignment. This condition is evaluated at different values of angular misalignments, as presented in Fig. 6.

The angular misalignment effect is presented by maintaining the same principal and cross-coupling DP in each plot. It is obvious from the graphs that angular misalignment affects the stability condition, as the angular misalignment increases the stability region increases accordingly.

The stability conditions presented by Eqs. (46) and (47) indicate that change in the angular misalignment α changes the stability region, the square of α is multiplied by one of the coupling DP. Eq. (47) can be simplified further to focus on the effect of the angular misalignment as

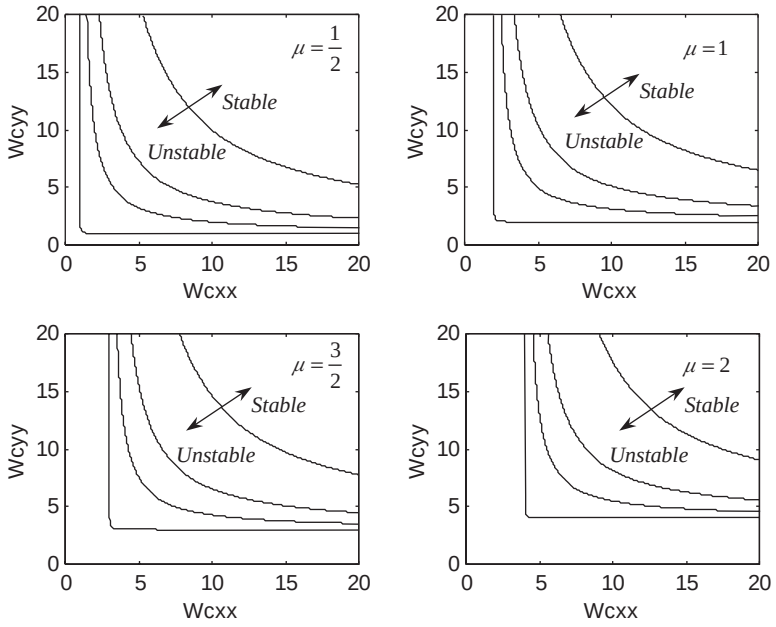

Fig. 5. Effect of μ on the threshold stability, Eq. (43).

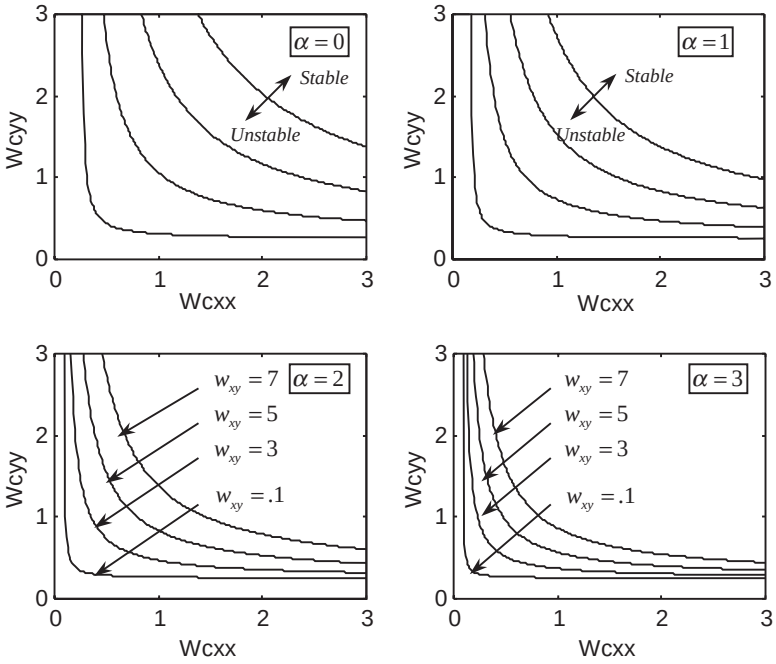

Fig. 6. Effect of angular misalignmentα, Eq. (45).

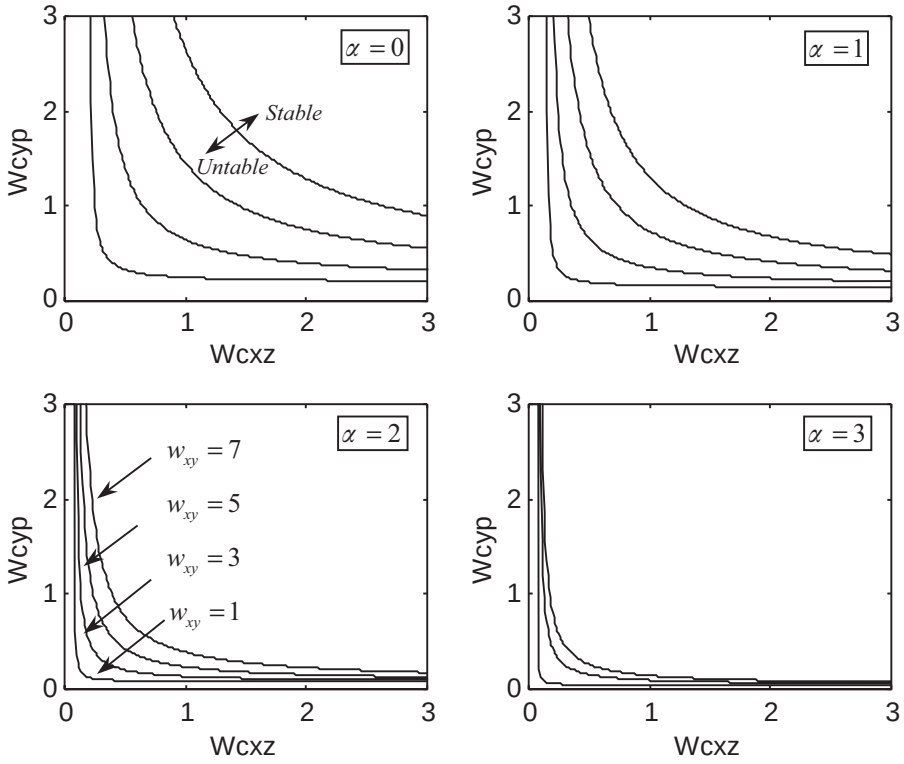

Fig. 7. Angular misalignment effects, Eq. (47).

$(Wcyp - 2\mu/\lambda)(Wcxz - 2\mu/\lambda) = (Wxy/\lambda)^2$, where

$$Wcyp = \left(\frac{\omega_{yy}^2}{\Omega^2}\right) + 2\alpha^2\left(\frac{\omega_{cy}^2}{\Omega^2}\right) + 4\left(\frac{\omega_{c\phi}^2}{\Omega^2}\right), \quad \frac{\omega_{yy}^2}{\Omega^2} = \frac{\omega_{cy}^2}{\Omega^2} = \frac{\omega_{c\phi}^2}{\Omega^2},$$

$$Wcxz = \left(\frac{\omega_{xx}^2}{\Omega^2}\right) + 2\alpha^2\left(\frac{\omega_{cz}^2}{\Omega^2}\right) + 4\left(\frac{\omega_{c\theta}^2}{\Omega^2}\right), \quad \frac{\omega_{xx}^2}{\Omega^2} = \frac{\omega_{cz}^2}{\Omega^2} = \frac{\omega_{c\theta}^2}{\Omega^2}, \quad Wxy = \frac{(\omega_{xy}^2 + \omega_{yx}^2)}{2\Omega^2}$$

and $\lambda = (5 + 2\alpha^2)$.

Fig. 7 consists of four different graphs, each for different values of misalignments, as indicated. The graphs show that an increase of the angular misalignment magnitude leads to an increase in the stability region, while keeping the DP the same. Angular misalignment reduces the cross-coupling term Wxy and for the stability condition threshold $2\mu/\lambda$ at the same time, both of which tend to improve stability. Should the polar moment of inertia be neglected the dimensionless variable μ becomes zero and the stability threshold coincide with the zero axis.

Fig. 8 presents the stability surface threshold for the condition of Eq. (47). The graph is generated for different values of α, making the dimensionless term $\mu = \frac{1}{2}$. The system is stable for values inside the stability surface. As the combined coupling and bearing principal stiffness terms increase the system becomes more stable. The four plots are for different values of angular

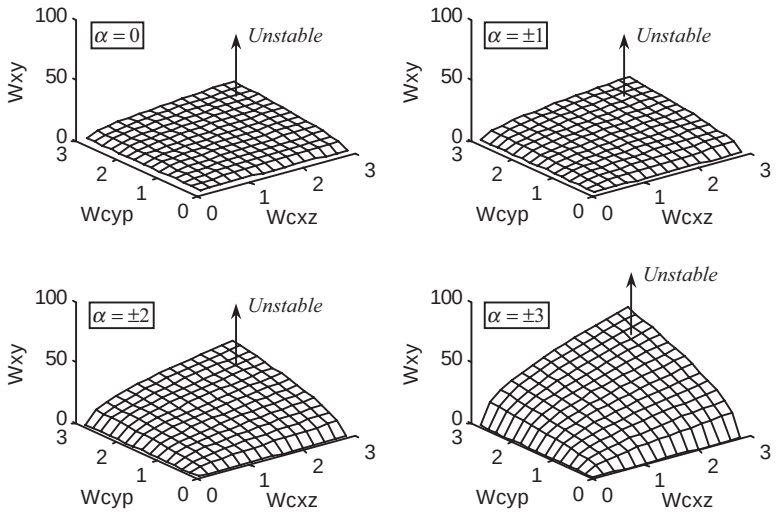

Fig. 8. Stability surface of Eq. (47) for different angular misalignment.

misalignment magnitudes, as indicated in the graphs. Increasing the angular misalignment magnitude tends to increase the volume of the stability region.

4. Conclusions

In this study, the effect of angular misalignment of two rigid rotors connected through a flexible mechanical coupling has been presented. The model consists of two rigid rotors coupled through a flexible mechanical coupling, a rigid mass attached at the middle of each rotor. Each rotor is mounted on two sets of hydrodynamic bearing that exhibit asymmetric principal stiffness and cross-coupling terms. The system degrees of freedom are the six orthogonal lateral deflections and the six angular rotations, which permits to inclusion of gyroscopic effects.

The system kinetic, potential, and dissipation energies are derived. Due to the non-linearity of the system, stability criteria are obtained using Liapunov's direct method through successive partial derivation of the Hamiltonian, which is obtained from the kinetic and potential energies. The conditions for sufficient stability of the system are derived through the check of positive definiteness of the resultant Hamiltonian matrix. The closed form whirl stability conditions are presented in terms of dimensionless stability parameters for generalization purpose. The dimensionless stability criteria, presented in graphical form clearly show that angular misalignment and coupling stiffness play a major role on the whirl stability of the system under study. As the angular misalignment or coupling stiffness terms increase, the stability regions increase accordingly.

Acknowledgements

The author acknowledges the support of Saudi ARAMCO, Saudi Arabia.

Appendix A. Nomenclature

a	shaft overhung
c_{xx}	bearing principal damping, x direction
c_{yy}	bearing principal damping, y direction
c_{xy}, c_{yx}	bearing cross-coupling damping terms
D	energy dissipation
H	Hamiltonian matrix
I_{Dp}	transverse moment of inertia for disk p
I_{Pp}	polar moment of inertia for disk p
$\mathbf{i}_p$	unit vector in the x_p direction
$\mathbf{j}_p$	unit vector in the y_p direction
$\mathbf{k}_p$	unit vector in the z_p direction
k_{ij}	stiffness element
k_{xx}	bearing principal stiffness, x direction
k_{yy}	bearing principal stiffness, y direction
k_{xy}, k_{yx}	bearing cross-coupling stiffness terms
k_{cx}	coupling stiffness, x direction
k_{cy}	coupling stiffness, y direction
k_{cz}	coupling stiffness, z direction
$k_{c\phi}$	coupling stiffness, ϕ direction
$k_{c\theta}$	coupling stiffness, θ direction
$k_{c\beta}$	coupling stiffness, β direction
l_p	bearing span of rotor p
m_p	mass p attached to rotor p
p	subscript indicates rotor 1 or 2
$\mathbf{Q}$	matrix
$\mathbf{Q}^*$	dimensionless matrix
$\mathbf{q}$	generalized co-ordinate
$\mathbf{r}_{b1p}$	position vector of bearing 1 of rotor p
$\mathbf{r}_{b2p}$	position vector of bearing 1 of rotor p
$\mathbf{r}_{mp}$	position vector of mass p of rotor p
$\mathbf{r}_{cp}$	position vector of coupling half of rotor p
$\mathbf{r}_{mp}$	velocity vector of mass p of rotor p
T	kinetic energy
U	remaining terms of Hamiltonian matrix
V	potential energy
x_p	x displacement of mass p
$\dot{x}_p$	x velocity of mass p
y_p	y displacement of mass p
$\dot{y}_p$	y velocity of mass p
z_p	z displacement of mass p
$\dot{z}_p$	z velocity of mass p
α	angular misalignment magnitude

ϕ angular displacement in x direction
θ angular displacement in y direction
β angular displacement in z direction
$\dot{\phi}$ angular velocity in x direction
$\dot{\theta}$ angular velocity in y direction
$\dot{\beta}$ angular velocity in z direction
Ω rotating speed

References

[1] J. Mancuso, General purpose vs. special purpose couplings, Proceeding of the Fifth Turbomachinery Symposium, Texas, 1995, pp. 167–177.
[2] H. Lorenzen, E.A. Niedermann, W. Wattinger, Solid couplings with flexible intermediate shafts for high speed turbo compressor trains, Proceeding of the 18th Turbomachinery Symposium, Texas, 1989, pp. 101–110.
[3] R.M. Rosenberg, On the dynamical behavior of rotating shafts driven by universal (Hooke) coupling, Journal of Applied Mechanics (1958) 47–51.
[4] K.M. Al-Hussain, I. Redmond, Dynamic response of two rotors connected by rigid mechanical coupling with parallel misalignment, Journal of Sound and Vibration 249 (3) (2002) 483–498.
[5] A.S. Sekhar, B.S. Prabhu, Effects of coupling misalignment on vibration of rotating machinery, Journal of Sound and Vibration (1995) 655–671.
[6] M. Xu, R.D. Marangoni, Vibration analysis of a motor-flexible coupling-rotor system subject to misalignment and unbalance, Part I: theoretical model analysis, Journal of Sound and Vibration (1994) 663–679.
[7] M. Saigo, Y. Okada, K. Ono, Self-excited vibration caused by internal friction in universal joins and its stabilizing method, Transaction of the American Society of Mechanical Engineers, Journal of Vibration and Acoustics 119 (1997) 221–229.
[8] J.L. Nikolajsen, The effect of misalignment on rotor vibrations, Journal of Engineering for Gas Turbines Power 120 (1998) 635–640.
[9] C.O. Chang, J.W. Cheng, Non-linear dynamics and instability of a rotating shaft-disk system, Journal of Sound and Vibration 160 (3) (1991) 433–454.
[10] J.M. Vance, Rotordynamic of Turbomachinery, Wiley, New York, 1988.
[11] Stroh, C.G., Rotordynamic stability—a simplified approach, Proceedings of the 14th Turbomachinery Symposium.
[12] J.C. Nicholos, R.G. Kirk, Selection and design of tilting pad and fixed lobe journal bearings for optimum turborotor dynamics, Proceedings of The Eighth Turbomachinery Symposium, 1979, pp. 43–57.
[13] J.W. Lund, Stability and damped critical speeds of a flexible rotor in fluid-film bearings, Transactions of the American Society of Mechanical Engineers, Journal of Engineering for Industry 96 (1974) 509–517.
[14] A.D. Dimarogonas, S. Haddad, Vibration for Engineers, Prentice-Hall, Englewood Cliffs, NJ, 1992.
[15] A.A. El-Marhomy, A.L. Schlack Jr., Dynamic stability of elastic rotor-bearing systems via Liapunov's direct method, Transaction of the American Society of Mechanical Engineers, Journal of Applied Mechanics 58 (1991) 1056–1063.
[16] A.A. El-Marhomy, Parametric stability analysis of rotor-bearing systems, Proceeding of the National Science Council ROC(A) 23 (1) (1999) 42–49.
[17] L. Meirovitch, Elements of Vibration Analysis, McGraw-Hill, Boston, 1986.
[18] R.H. Badgley, J.F. Booker, Turborotor instability: effect of initial transient on plane motion, Transaction of American Society of Mechanical Engineers, Journal of Lubrication Technology (1969) 625–633.